EXTENDED DATA FIGURE LEGENDS

Extended Data Figure 1. IECs from HDAC3$^{\Delta IEC}$ mice demonstrate alterations in gene expression coupled with increased histone acetylation. (a, b) HDAC3 expression in IECs from HDAC3^{FF} or HDAC3$^{\Delta IEC}$ mice by **(a)** real-time PCR and **(b)** Western analysis. **(c)** Purity of sort-purified EpCAM^{+} IECs. **(d)** Gene-set enrichment analysis (GSEA) comparing IECs from HDAC3^{FF} and HDAC3$^{\Delta IEC}$ mice to published data enrichment sets obtained from the Molecular Signatures Database. **(e)** Heat map of H3K9Ac signal in IECs from HDAC3^{FF} and HDAC3$^{\Delta IEC}$ mice at genes that are upregulated in IECs of HDAC3$^{\Delta IEC}$ mice. Each row represents a single gene sorted by the peak heights in the HDAC3$^{\Delta IEC}$ mice. H3K9Ac signals were normalized to reads per kilobase per 10 million mapped reads. **(f)** ChIP-qPCR comparing H3K9Ac levels in IECs from HDAC3$^{\Delta IEC}$ mice versus HDAC3^{FF} mice at promoter regions of select upregulated genes. Data are presented as fold difference relative to control HDAC3^{FF} IECs. *n*=3 mice per group. *p<0.05.

Extended Data Figure 2. HDAC3$^{\Delta IEC}$ mice exhibit altered IEC homeostasis. (a) Representative H&E (left) and lysozyme (right) stained sections of small intestine from 18 day old HDAC3^{FF} and HDAC3$^{\Delta IEC}$ mice. Bars, 50mm. **(b)** Immunohistochemistry for active caspase-3 in small intestinal crypts from HDAC3^{FF} and HDAC3$^{\Delta IEC}$ mice. Arrows indicate positive nuclear staining. Bars, 50mm**.** **(c)** Electron micrograph of littermate HDAC3^{FF} and HDAC3$^{\Delta IEC}$ Paneth cells. Bars, 2mm. **(d)** Immunohistochemistry for Ki-67 in colonic crypts from HDAC3^{FF} and HDAC3$^{\Delta IEC}$ mice. Bars, 50mm.

Extended Data Figure 3. HDAC3$^{\Delta IEC}$ mice demonstrate impaired intestinal barrier function, spontaneous intestinal inflammation, and defective anti-bacterial defenses. **(a)** FITC levels in plasma assessed 4 hours after oral gavage with FITC-dextran (0.6mg/gm) of HDAC3^{FF} (*n*=3) and HDAC3$^{\Delta IEC}$ (*n*=5) mice and presented as fold difference relative to HDAC3^{FF} mice. **(b)** Bactericidal activity against *Salmonella typhimurium* of supernatants from carbamyl choline (CCh)-stimulated small intestinal crypts. Data are presented as % killing compared to unstimulated crypts. *n*=4 mice per group. (**c)** Daily changes in body weight following oral infection with *L. monocytogenes.* **(d)** Colony forming units (CFU) of *L. monocytogenes* grown on LB plates containing streptomycin from mesenteric lymph nodes (mLN) 72 hours post-infection. HDAC3^{FF} (*n*=9) and HDAC3$^{\Delta IEC}$ (*n*=7). **(e)** Rectal prolapse in a 4 month old HDAC3$^{\Delta IEC}$ mouse. **(f)** Representative H&E stained section of colons, **(g)** quantification of CD4^{+} and CD19^{+} cells (gated live, CD45^{+}) in lamina propria, and **(h)** disease score from mice in (e). Bars, 50mm. Data depicted are from two pooled experiments.*p<0.05. **p<0.01.

Extended Data Figure 4. HDAC3$^{\Delta LysM}$ mice do not demonstrate increased sensitivity to DSS-induced intestinal damage and inflammation. **(a)** Daily changes in body weight,**(b)** disease score, **(c)** colon length and **(d)** representative H&E stained large intestine sections of 2.5% DSS-treated HDAC3^{FF} and HDAC3$^{\Delta LysM}$ mice. Bars, 50mm. *n*=4 mice per group. Data are representative of two independent experiments.

Extended Data Figure 5. HDAC3$^{\Delta IEC\text{-}IND}$ mice exhibit Paneth cell loss and impaired

barrier function following tamoxifen-induced deletion of HDAC3 in IECs. (a) HDAC3$^{\Delta IEC\text{-}IND}$ mice contain the floxed HDAC3 gene and a tamoxifen-dependent Cre recombinase (Cre-ER^{T2}) controlled by the *Villin* promoter. **(b, c)** HDAC3 expression in IECs from HDAC3^{FF} and HDAC3$^{\Delta IEC\text{-}IND}$ mice by **(b)** real-time PCR and **(c)** Western analysis after tamoxifen treatment. **(d)** Representative H&E (top) and active caspase-3 (bottom) stained sections of small intestine of HDAC3$^{\Delta IEC\text{-}IND}$ mice treated with either vehicle or tamoxifen for three 5 day periods over 30 days. Arrows indicate dead cell (top) and positive nuclear staining (bottom). Bars, 50mm. **(e)** Albumin measured by ELISA from fecal samples harvested from the same mice prior to tamoxifen-induced HDAC3 deletion (-) and following tamoxifen-induced deletion (+). **(f)** FITC levels in plasma assessed 4 hours after oral gavage. HDAC3^{FF}(*n*=3), HDAC3$^{\Delta IEC\text{-}IND}$ (*n*=8). Data are representative of two independent experiments. *p< 0.05, **p<0.01.

Extended Data Figure 6. HDAC3$^{\Delta IEC\text{-}IND}$ mice exhibit exhibit enhanced susceptibility to DSS-induced intestinal damage and inflammation. (a) Representative large intestine and **(b)** colon length (% naive) after 5 days of 2.5% DSS. **(c)** Frequencies of neutrophils (CD11b^{+} Ly6G^{+}) and macrophages (CD11b^{+} Ly6G^{-}) in the colonic lamina propria. **(d)** Representative H&E stained intestine sections of HDAC3^{FF} and HDAC3$^{\Delta IEC\text{-}IND}$ mice. Bars, 50mm. *n*=4 mice per group. Data are representative of four independent experiments. **p<0.01.

Extended Data Figure 7. Inhibition of IEC-intrinsic HDAC3 results in temporal and spatial alterations in the diversity of intestinal commensal bacteria. (a) Average

679 UniFrac distance between HDAC3^{FF} mice and HDAC3$^{\Delta IEC}$ mice, or HDAC3^{FF} and
680 HDAC3$^{\Delta IEC}$ based on 16S rRNA gene sequences determined from stool bacterial
681 communities collected three times over a 4 week period from adult HDAC3^{FF} and
682 HDAC3$^{\Delta IEC}$ mice. **(b)** Phylum level comparison of stool bacterial communities at each
683 time point. **(c)** Phylum level comparison of bacterial communities in contents from small
684 (SI) or large intestine (LI). **(d)** Average UniFrac distance between HDAC3^{FF} mice and
685 HDAC3$^{\Delta IEC\text{-}IND}$ mice, or within HDAC3^{FF} and HDAC3$^{\Delta IEC\text{-}IND}$ groups based on 16S
686 rRNA gene sequences determined from stool bacterial communities collected prior to
687 tamoxifen induction (Pre) and 15 days following 5 days of tamoxifen administration
688 (Post). **(e)** Principal coordinate analysis of samples in (a). *n*=3 mice per group. *p< 0.05,
689 **p<0.01.
690
691 **Extended Data Figure 8. HDAC3-dependent regulation involves integration of**
692 **commensal bacteria-derived signals.** Functional classification of enriched pathways by
693 DAVID pathway analysis using genes represented in Figure 4a.
694
695 **Extended Data Figure 9. Epithelial HDAC3 integrates commensal bacteria-derived**
696 **signals to establish commensalism and maintain tissue homeostasis. (a)** In the
697 healthy HDAC3-sufficient intestine, HDAC3-dependent maintenance of intestinal
698 homeostasis reflects an integrated effect of commensal-derived signals and host
699 transcriptional networks. **(b)** Impaired IEC-intrinsic HDAC3-dependent gene regulation
700 results in increased IEC proliferation, altered Paneth cell survival, intestinal dysbiosis,
701 impaired intestinal barrier function and increased susceptibility to intestinal damage and

inflammation.

Extended Data Figure 10. Pyrosequencing parameters. (a) Number of reads and alpha diversity (observed species). **(b)** Rarefaction curves. **(c)** Principal coordinate analysis 2D plots. **(d)** Hierarchical clustering dendrograms.

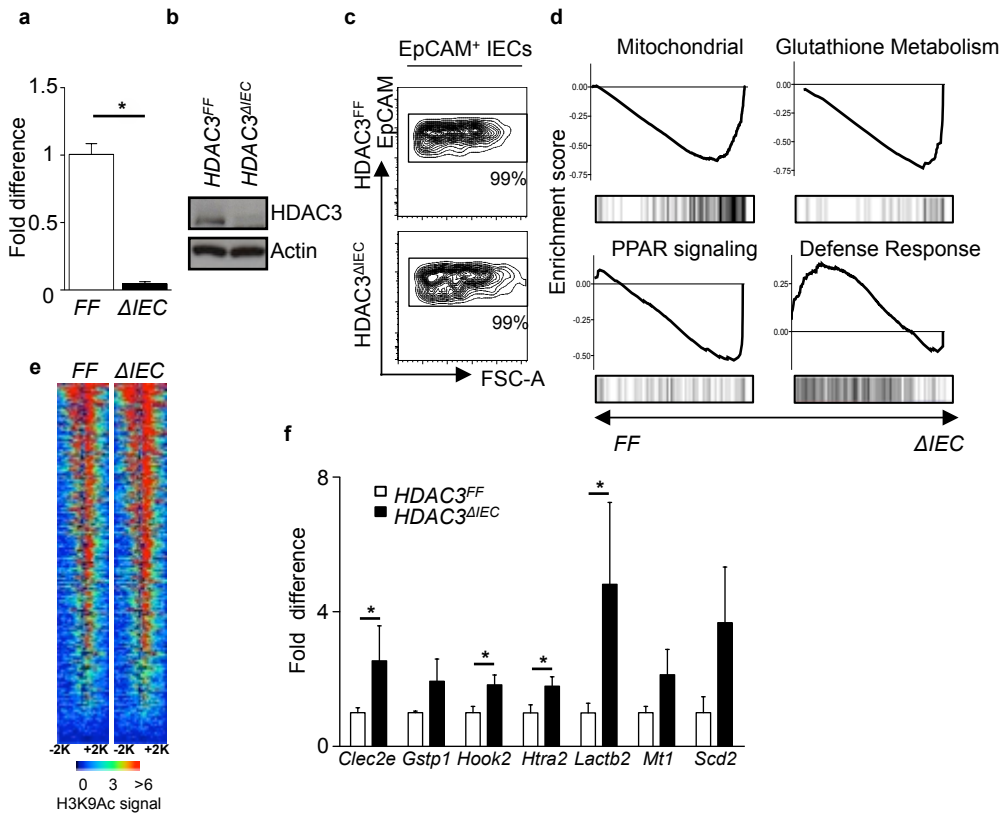
a
b
c
d
Fold difference
1.5
1
0.5
0
*
FF
ΔIEC
HDAC3FF
HDAC3ΔIEC
HDAC3
Actin
EpCAM+ IECs
HDAC3FF EpCAM
99%
HDAC3ΔIEC
99%
FSC-A
Mitochondrial
Glutathione Metabolism
PPAR signaling
Defense Response
Enrichment score
FF
ΔIEC
e
FF
ΔIEC
-2K
+2K
-2K
+2K
0
3
>6
H3K9Ac signal
f
HDAC3FF
HDAC3ΔIEC
Fold difference
8
4
0
Clec2e
Gstp1
Hook2
Htra2
Lactb2
Mt1
Scd2

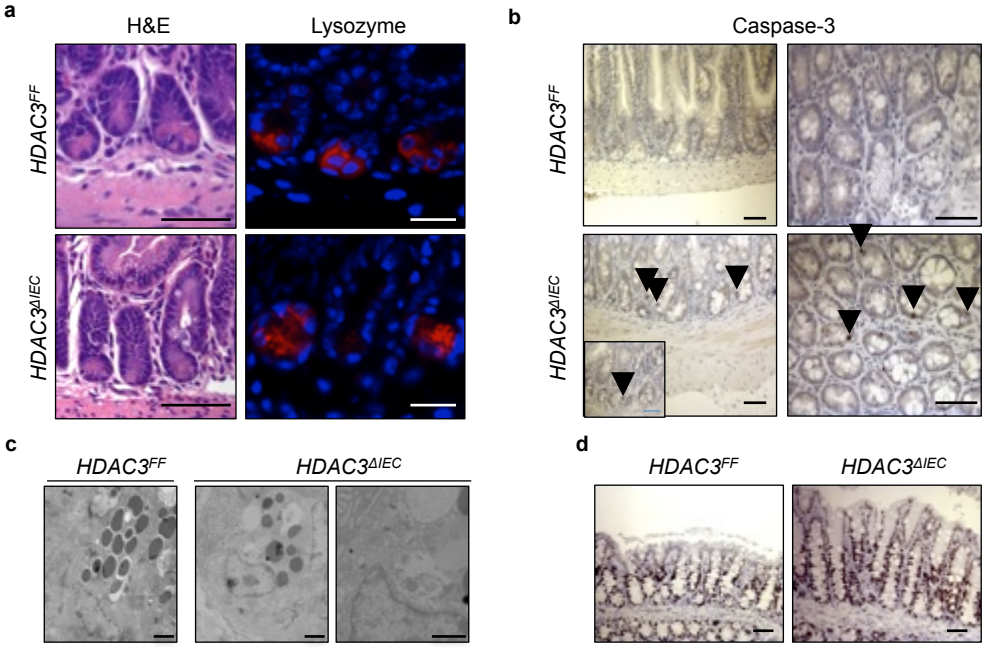
a
H&E
Lysozyme
HDAC3FF
HDAC3ΔIEC
b
Caspase-3
HDAC3FF
HDAC3ΔIEC
c
HDAC3FF
HDAC3ΔIEC
d
HDAC3FF
HDAC3ΔIEC

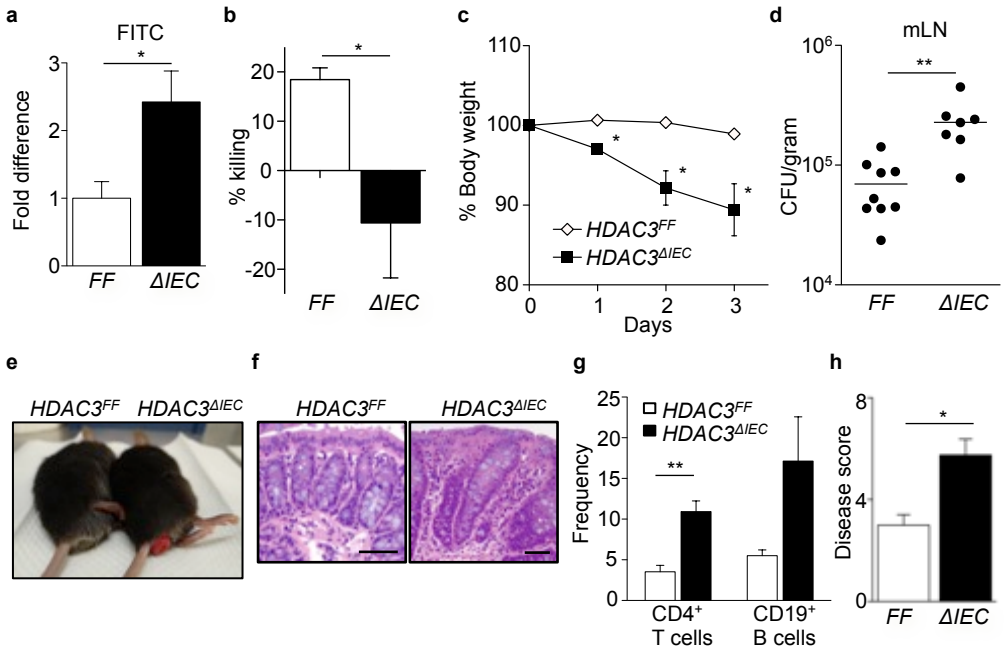
a
FITC
Fold difference
FF
ΔIEC
b
% killing
FF
ΔIEC
c
% Body weight
Days
HDAC3FF
HDAC3ΔIEC
d
mLN
CFU/gram
FF
ΔIEC
e
HDAC3FF
HDAC3ΔIEC
f
HDAC3FF
HDAC3ΔIEC
g
Frequency
HDAC3FF
HDAC3ΔIEC
CD4+ T cells
CD19+ B cells
h
Disease score
FF
ΔIEC

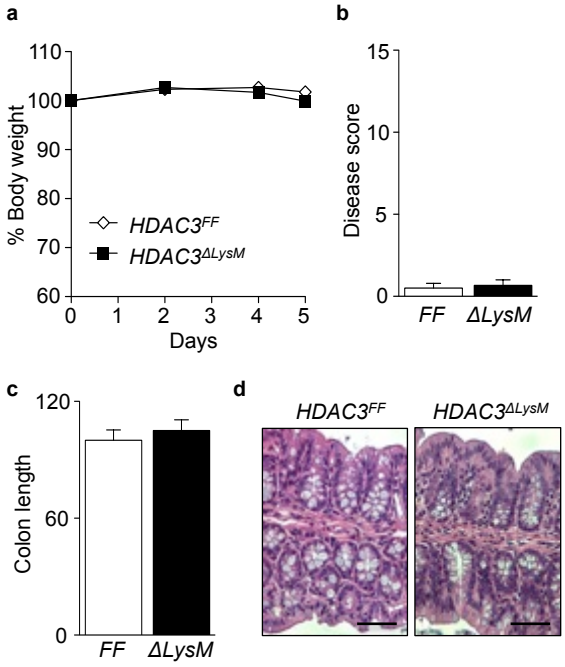
a
b
c
d
% Body weight
Days
HDAC3FF
HDAC3ΔLysM
Disease score
FF
ΔLysM
Colon length
HDAC3FF
HDAC3ΔLysM

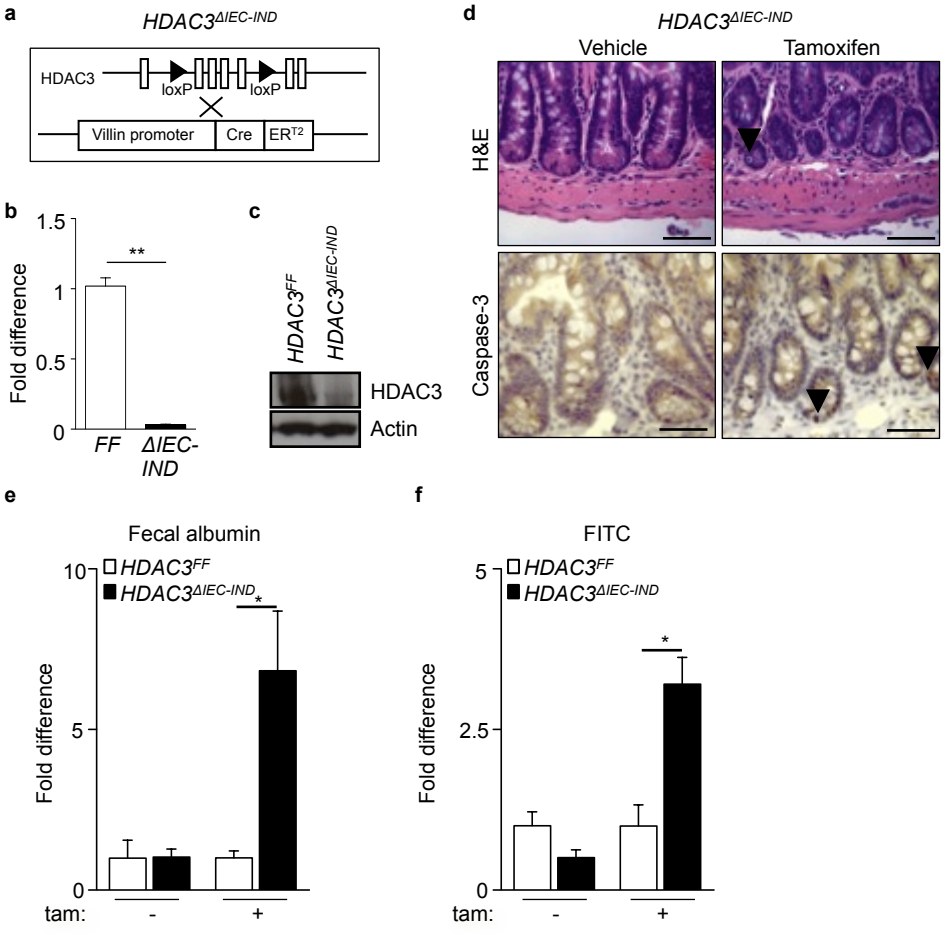
a
HDAC3ΔIEC-IND
HDAC3
loxP
loxP
Villin promoter
Cre
ERT2
b
Fold difference
1.5
1
0.5
0
**
FF
ΔIEC-IND
c
HDAC3FF
HDAC3ΔIEC-IND
HDAC3
Actin
d
HDAC3ΔIEC-IND
Vehicle
Tamoxifen
H&E
Caspase-3
e
Fecal albumin
HDAC3FF
HDAC3ΔIEC-IND
*
Fold difference
10
5
0
tam:
-
+
f
FITC
HDAC3FF
HDAC3ΔIEC-IND
*
Fold difference
5
2.5
0
tam:
-
+

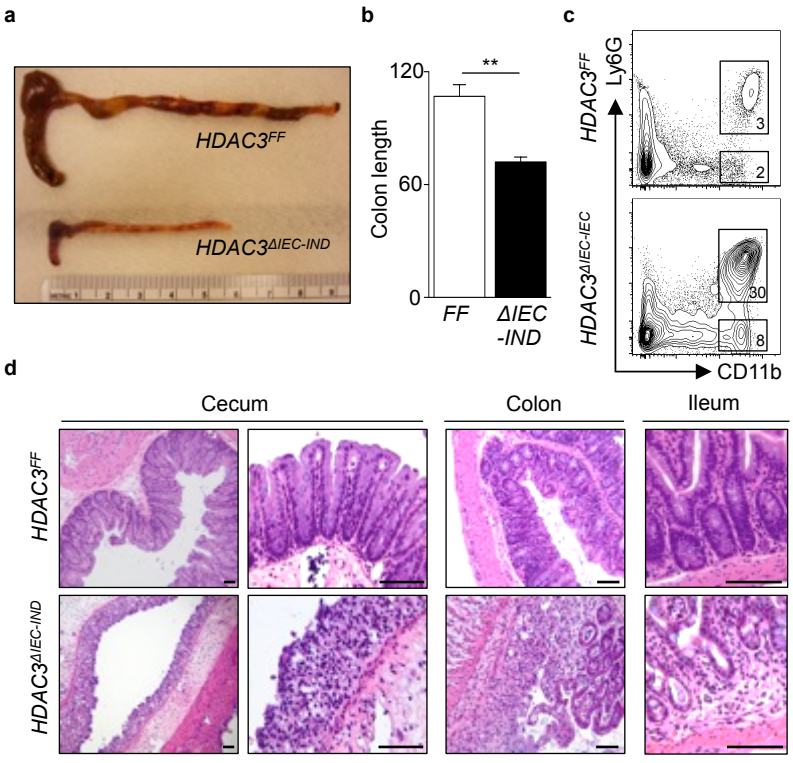
a
HDAC3FF
HDAC3ΔIEC-IND
b
120
60
0
Colon length
**
FF
ΔIEC
-IND
c
HDAC3FF
Ly6G
3
2
HDAC3ΔIEC-IEC
30
8
CD11b
d
Cecum
Colon
Ileum
HDAC3FF
HDAC3ΔIEC-IND

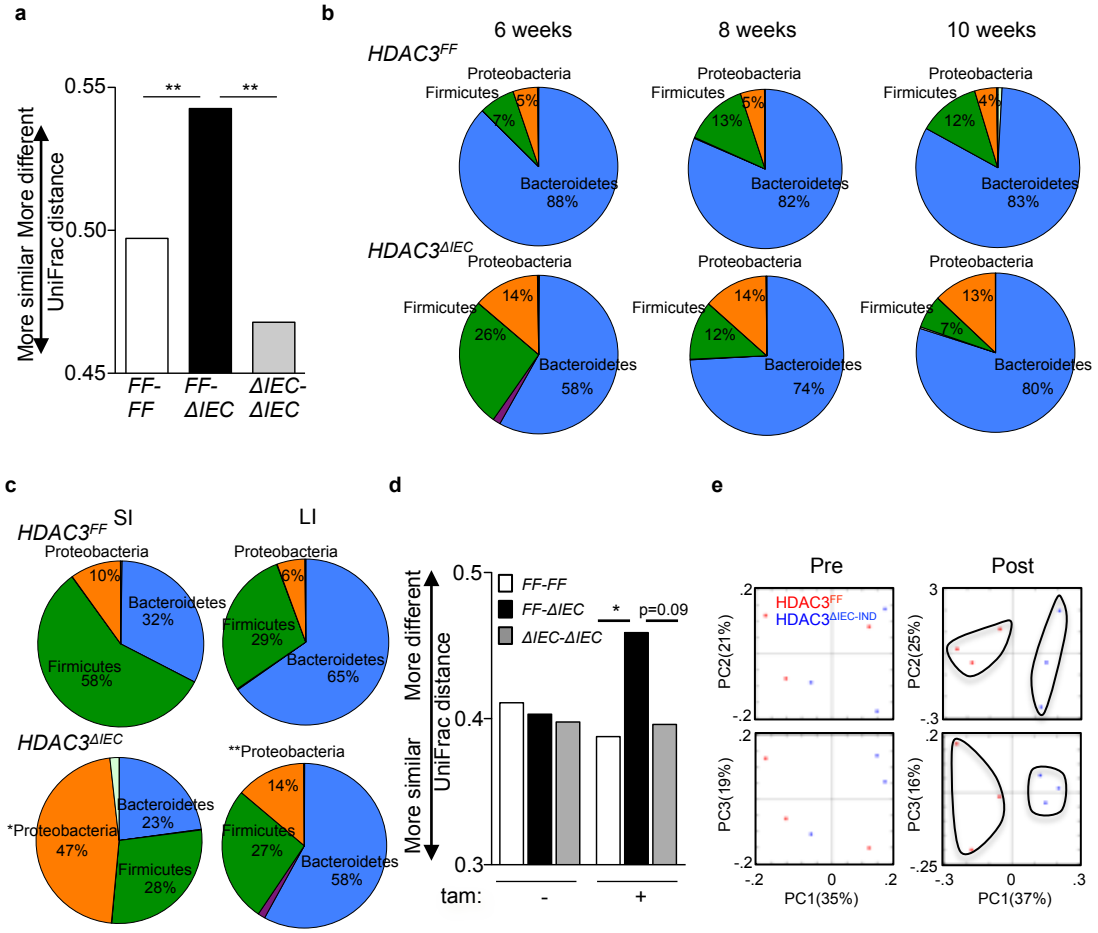
a
b
c
d
e
More similar More different
UniFrac distance
0.55
0.50
0.45
**
**
FF-FF
FF-ΔIEC
ΔIEC-ΔIEC
6 weeks
8 weeks
10 weeks
HDAC3FF
HDAC3ΔIEC
Proteobacteria
Firmicutes
Bacteroidetes
5%
7%
88%
5%
13%
82%
4%
12%
83%
14%
26%
58%
14%
12%
74%
13%
7%
80%
SI
LI
10%
32%
58%
6%
29%
65%
*Proteobacteria
**Proteobacteria
47%
23%
28%
14%
27%
58%
0.5
0.4
0.3
FF-FF
FF-ΔIEC
ΔIEC-ΔIEC
*
p=0.09
tam:
-
+
Pre
Post
HDAC3FF
HDAC3ΔIEC-IND
PC2(21%)
PC2(25%)
PC3(19%)
PC3(16%)
PC1(35%)
PC1(37%)

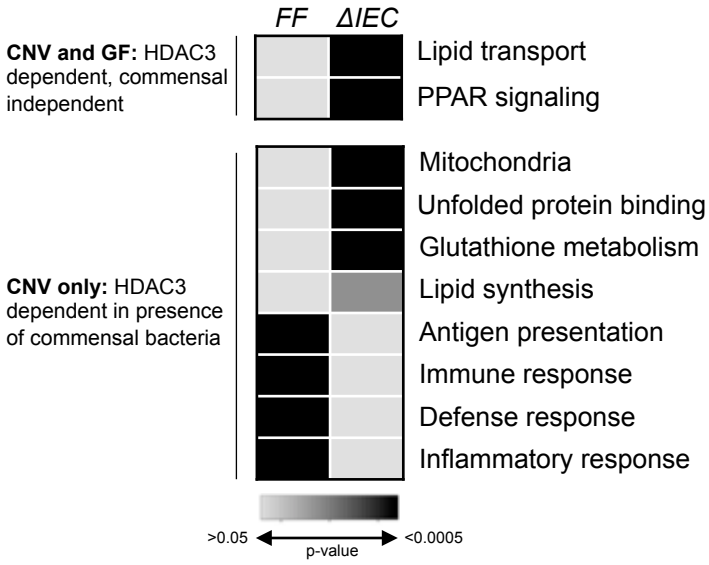
FF
ΔIEC
CNV and GF: HDAC3 dependent, commensal independent
Lipid transport
PPAR signaling
CNV only: HDAC3 dependent in presence of commensal bacteria
Mitochondria
Unfolded protein binding
Glutathione metabolism
Lipid synthesis
Antigen presentation
Immune response
Defense response
Inflammatory response
>0.05
<0.0005
p-value

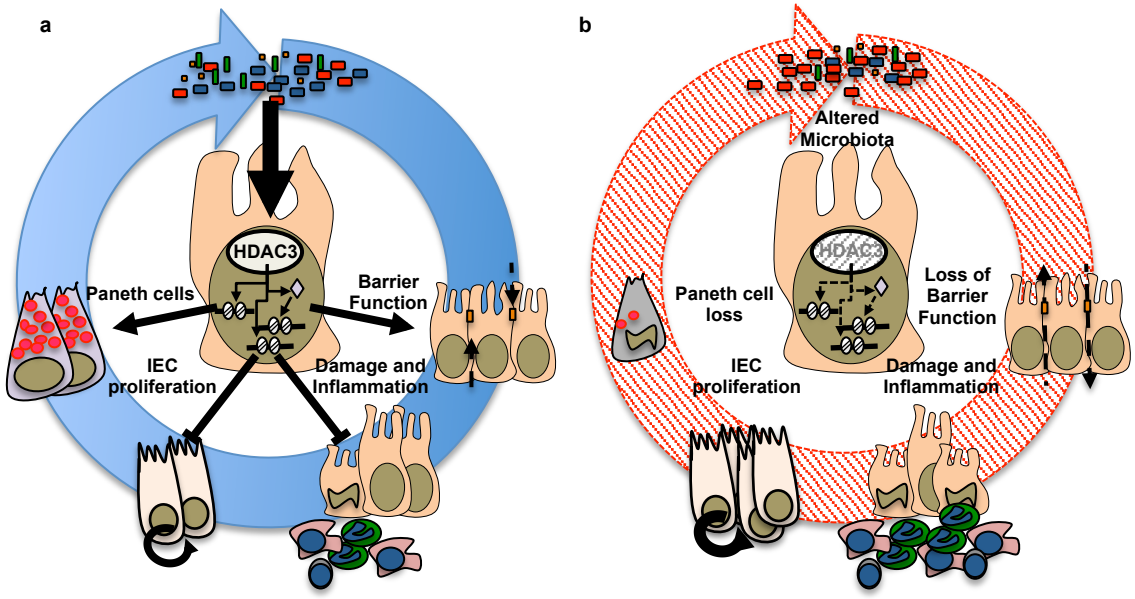
a
HDAC3
Paneth cells
Barrier
Function
IEC
proliferation
Damage and
Inflammation
b
Altered
Microbiota
HDAC3
Paneth cell
loss
Loss of
Barrier
Function
IEC
proliferation
Damage and
Inflammation

a

Genotype	Timepoint/ Location	Average reads	Average obs species
FF	6 weeks	4199	174
ΔIEC	6 weeks	2858	152
FF	8 weeks	3333	233
ΔIEC	8 weeks	3179	147
FF	10 weeks	1714	147
ΔIEC	10 weeks	2476	95
FF	LI	2368	231
ΔIEC	LI	1156	177
FF	SI	3641	71
ΔIEC	SI	2758	43
FF	Pre	2253	351
ΔIEC-IND	Pre	2319	308
FF	Post	2624	363
ΔIEC-IND	Post	1611	230

b

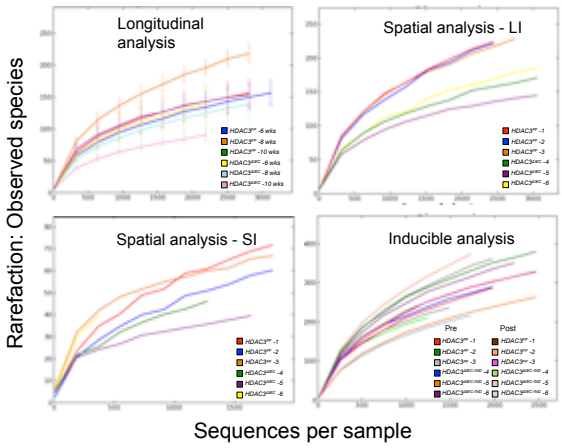

c

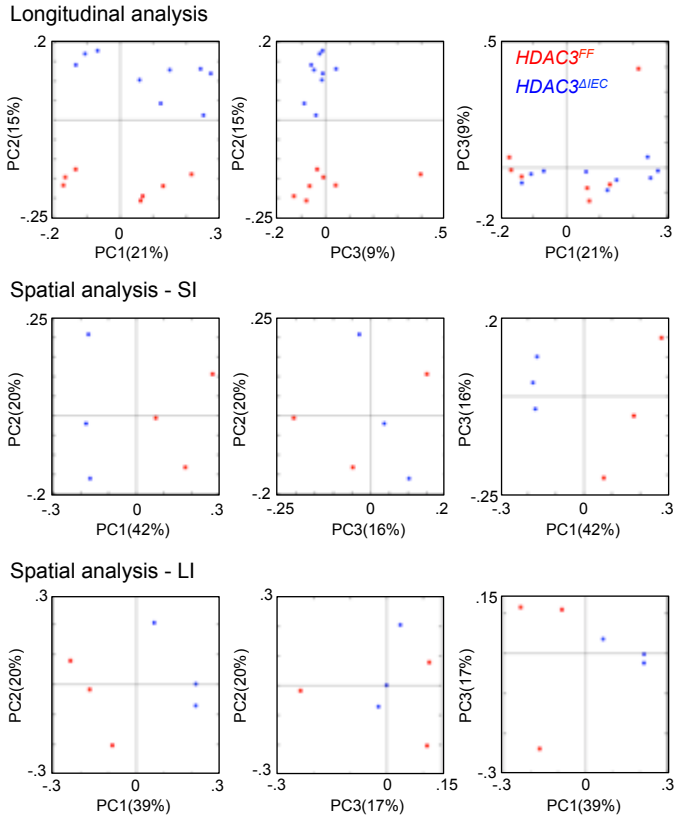

d